Mineralogical Magazine, February 2000, Vol. 64(1), pp. 25–30

Arizona porphyry copper/hydrothermal deposits I. The structure of chenevixite and luetheite

P. C. BURNS[1,*], J. V. SMITH[2] AND I. M. STEELE[2]

[1] Department of Civil Engineering and Geological Sciences, University of Notre Dame, 156 Fitzpatrick, Notre Dame, IN 46556, U.S.A.
[2] Department of Geophysical Sciences, University of Chicago, Chicago, IL 60637, U.S.A.

ABSTRACT

The crystal structure of chenevixite, $Cu_2M_2(AsO_4)_2(OH)_4$ (where $M = Fe^{3+}$ or Al), pseudo-orthorhombic, monoclinic, a = 5.7012(8), b = 5.1801(7), c = 29.265(2) Å, β = 89.99(1)°, V = 864.3(4) Å^3, space group $B12_11$, Z = 4, was solved by direct methods and refined by least-squares techniques to R = 8.4% and a goodness-of-fit (S) of 1.37 for 1176 unique observed ($F \geqslant 4\sigma_F$) reflections collected for a twinned microcrystal using graphite-monochromated Mo-$K\alpha$ X-rays and a CCD area detector. Vertex- and edge-sharing arsenate tetrahedra, $Al\phi_6$ octahedra, and Jahn-Teller-distorted $Cu^{2+}\phi_6$ octahedra [ϕ: O^{2-}, $(OH)^-$] form a framework unique from those in Cu^{2+} oxysalt minerals. Chains of edge-sharing $Cu^{2+}\phi_6$ octahedra, with $Al\phi_6$ octahedra attached on opposing sides by the sharing of edges, are linked into layers parallel to (001) by sharing vertices with AsO_4 tetrahedra, and the layers are linked to form a framework by the sharing of polyhedral elements between adjacent $Al\phi_6$ octahedra, as well as between AsO_4 tetrahedra and $Al\phi_6$ octahedra.

KEYWORDS: chenevixite, luetheite, Cu oxysalt, structure determination, CCD detector.

Introduction

CHENEVIXITE, defined as $Cu_2Fe_2(AsO_4)_2(OH)_4(H_2O)$, and luetheite, defined as $Cu_2Al_2(AsO_4)_2(OH)_4(H_2O)$, occur as microcrystals in veinlets and vugs in rhyolite porphyry from the Humbolt mine, Santa Cruz County, Arizona (Williams, 1977). The similar diffraction data and physical properties indicated that luetheite is isostructural with chenevixite. Recently, the introduction of CCD-based detectors for X-rays has made it possible to obtain data for much smaller crystals than was possible with conventional techniques (Burns, 1998). A CCD-based detector was used to collect data for a supposed single crystal of chenevixite, which turned out to be a mixture of chenevixite and luetheite. This paper is the first in a series concerning the crystal structures of Cu^{2+} oxysalts from hydrothermal deposits in Arizona.

* E-mail: pburns@nd.edu

Experimental

X-ray data

The crystal, from a specimen collected at the Humboldt mine, Patagonia, Arizona, was the largest (0.12 × 0.06 × 0.01 mm) that could be located. It exhibited sharp extinction between crossed polarizers and did not show twinning. Data were collected at the Environmental Mineralogy and Crystal Structures Laboratory at the University of Notre Dame. The crystal was mounted on a Bruker PLATFORM 3-circle goniometer equipped with a 1K SMART CCD (charge-coupled device) detector and a crystal-to-detector distance of 5 cm.

Data were collected using monochromatic Mo-$K\alpha$ X-radiation and frame widths of 0.3° in ω, with 60 s spent counting per frame. More than a hemisphere of three-dimensional data was collected to ~57°2θ. The final unit-cell dimensions (Table 1) were refined on the basis of 1332 reflections using least-squares techniques. Data were collected for $3° \leqslant 2\theta \leqslant 56.7°$ in approximately 23 h; comparison of the intensities of equivalent reflections

TABLE 1. Miscellaneous information on chenevixite

a (Å)	5.7012(8)	Crystal size (mm)	0.12 × 0.06 × 0.01
b (Å)	5.1801(7)		
c (Å)	29.265(2)	Total ref.	2098
β (°)	89.99(1)	Unique $\|F\| \geqslant 4\sigma_F$	1176
V (Å^3)	864.3(4)		
Space group	$B12_11$	Final R	8.4
		Final *S*	1.37

Unit cell contents 4[$Cu_2M_2(AsO_4)_2(OH)_4$], M = Al, Fe^{3+}
$R = \Sigma(|F_o|-|F_c|)/\Sigma|F_o|$
$S = [\Sigma w(|F_o|-|F_c|)^2/(m-n)]^{½}$, for m observations and n parameters

collected at different times during the data collection showed no evidence of significant decay. The three-dimensional data were integrated and corrected for Lorentz, polarization, and background effects using the Bruker program SAINT. An empirical absorption-correction was done using the program SADABS (G. Sheldrick, unpublished computer program). A total of 2098 reflections were collected; merging of equivalent reflections gave 1520 unique reflections (R_{int} = 6.4%) with 1176 classed as observed ($|F_o| \geqslant 4\sigma_F$).

Chemical analysis

A single crystal from the same specimen as the crystal used for the collection of the X-ray diffraction data was mounted in epoxy, polished, and coated with carbon. *In situ* chemical analyses were done in wavelength-dispersion spectroscopy (WDS) mode with a Cameca SX-50 electron microprobe at the University of Chicago. The operating voltage was 15 kV, and the beam current was 25 μA. Standards used for the electron-microprobe analysis were: anorthite for Al, synthetic $FeAs_2$, and Cu metal. H_2O was calculated from the stoichiometry obtained from the crystal-structure analysis. Electron-backscatter and X-ray images of the crystal showed that it was strongly zoned, and analysis confirmed the zoning corresponded to variations in Fe and Al. Nine analyses obtained along a line from edge to edge across the crystal are given in Table 2.

Structure solution and refinement

Scattering curves for neutral atoms, together with anomalous dispersion corrections, were taken from *International Tables for X-ray Crystallography, Vol. IV* (Ibers and Hamilton, 1974). The Bruker SHELXTL Version 5 system of programs was used for the determination and refinement of the crystal structure.

TABLE 2. Chemical analysis of chenevixite

	wt.%						per 12 anions				
Pt.	Fe_2O_3	Al_2O_3	As_2O_5	CuO	H_2O*	Total	Fe	Al	Fe+Al	As	Cu
1	5.47	16.1	43.6	27.1	6.72	99.0	0.37	1.69	2.06	2.03	1.83
2	23.2	1.8	38.0	26.0	5.92	94.9	1.77	0.21	1.98	2.01	1.99
3	26.7	1.0	38.3	26.4	6.11	98.5	1.97	0.12	2.09	1.96	1.96
4	23.2	2.8	39.7	26.5	6.18	98.4	1.69	0.32	2.01	2.01	1.94
5	20.3	5.2	40.8	26.9	6.34	99.5	1.44	0.58	2.02	2.02	1.92
6	16.6	8.5	40.7	27.8	6.47	100.1	1.16	0.93	2.08	1.97	1.95
7	14.9	9.7	41.1	27.9	6.52	100.1	1.03	1.05	2.08	1.98	1.94
8	15.1	9.3	42.1	27.4	6.55	100.4	1.04	1.00	2.04	2.02	1.90
9	14.7	8.2	42.8	27.0	6.44	99.1	1.03	0.90	1.93	2.08	1.90

* calculated on the basis of stoichiometry

Initial attempts to solve the structure used the primitive unit cell a = 14.908(2), b = 5.1826(6), c = 5.7011(6), β = 101.03(1)°. Systematic absences and reflection statistics were consistent with space group $P2_1$, and a structure model was obtained using direct methods. However, the model only refined to an agreement index (R) of 20%, with numerous significant electron-density peaks remaining in the difference-Fourier maps at locations that were incompatible with additional atomic sites. Examination of the observed and calculated structure factors revealed that the most significant deviations corresponded to $F_{obs} \gg F_{calc}$, suggesting that the crystal was twinned, and that the diffraction pattern corresponded to the superposition of two or more lattices. A re-examination of the raw data showed that the twinning, if present, involved complete overlap of the diffraction patterns that correspond to each twin component.

The transformation matrix [001/010/$\bar{2}0\bar{1}$] was applied to obtain the unconventional B-centred pseudo-orthorhombic unit cell with a = 5.701(1), b = 5.183(1), c = 29.265(2), β = 89.99(1) to facilitate a model that included the effects of twinning. The structure was solved in space group $B12_11$ using direct methods, and refined to an agreement index (R) of 20%. The twin law [100/0$\bar{1}$0/00$\bar{1}$] was applied and the structure was refined according to the method of Jameson *et al.* (1982) and Herbst-Irmer and Sheldrick (1998), resulting in a spectacular improvement of the R. The twin-component scale factor refined to 0.494(4), indicating the twins were present in identical proportions. The occupancies of the M sites (M = Al, Fe^{3+}) were refined using the atomic scattering factors for Fe and Al, with the total occupancy of each site constrained to be one. The final structure model gave an R of 8.4% and a goodness-of-fit (S) of 1.37 for 1176 observed reflections ($|F_o| \geqslant 4\sigma_F$). Final positional and displacement parameters are given in Table 3 and selected interatomic distances and angles in Table 4. Observed and calculated structure factors have been deposited with the editor of *Mineralogical Magazine* and are available upon request. They are also available in the online version of the journal (http://www.minersoc.org).

The structure refinement converged slowly because of twinning, the final R factor is higher than expected for a well behaved crystal, and there is a higher-than-normal uncertainty in the atomic positional parameters, which is reflected in the relatively large errors reported for the bond lengths. The displacement parameters for the anions show a large range, and may be unreliable

TABLE 3. Atomic coordinates* and displacement parameters ($\times 10^4$) for chenevixite

	x	y	z	*U_{iso}
As1	0.8760(6)	0.6865(4)	0.9385(1)	58(7)
As2	0.6176(7)	0.0923(5)	0.1886(1)	87(10)
M1	0.122(1)	0.3848(8)	0.2145(2)	74(13)
M2	0.625(1)	0.8860(8)	0.0343(2)	84(14)
Cu1	0.8659(9)	0.633(2)	0.1259(3)	92(6)
Cu2	0.366(1)	0.646(2)	0.1245(3)	100(6)
O1	0.857(3)	0.725(3)	0.9984(6)	111(41)
O2	0.617(4)	0.020(4)	0.2421(7)	231(52)
O3	0.865(3)	0.264(3)	0.1747(5)	29(34)
O4	0.155(4)	0.553(5)	0.9245(8)	474(74)
O5	0.886(4)	0.996(3)	0.9122(6)	241(48)
O6	0.611(4)	0.821(4)	0.1574(6)	175(46)
O7	0.646(4)	0.543(4)	0.9216(6)	238(52)
O8	0.388(4)	0.279(4)	0.1754(6)	125(44)
OH1	0.382(5)	0.552(4)	0.2555(7)	344(57)
OH2	0.620(4)	0.215(4)	−0.0003(7)	173(49)
OH3	0.115(3)	0.682(3)	0.1713(5)	87(36)
OH4	0.619(5)	0.549(4)	0.0808(7)	405(66)

* $U = U \times 10^4$

TABLE 4. Selected interatomic distances for chenevixite

As1−O7	1.59(2)	As2−O2	1.61(2)
As1−O5	1.78(2)	As2−O8	1.67(2)
As1−O1	1.77(2)	As2−O3	1.71(2)
As1−O4a	1.78(3)	As2−O6b	1.68(2)
<As1−O>	1.73	<As2−O>	1.67
*M*1−OH1	2.09(2)	*M*2−O4f	1.94(2)
*M*1−OH1c	1.93(2)	*M*2−OH2g	1.93(2)
*M*1−O2d	1.99(2)	*M*2−O1h	1.88(2)
*M*1−O3e	1.97(2)	*M*2−OH2i	1.98(2)
*M*1−O8	1.98(2)	*M*2−OH4	2.21(2)
*M*1−OH3	1.99(2)	*M*2−O7f	2.17(2)
<*M*1−ϕ>	1.99	<*M*2−ϕ>	2.02
Cu1−OH3a	1.96(2)	Cu2−O6	1.92(2)
Cu1−OH4	1.98(3)	Cu2−O5k	1.96(2)
Cu1−O6	1.98(2)	Cu2−OH4	1.99(3)
Cu1−O5j	1.93(2)	Cu2−OH3	1.99(2)
Cu1−O3	2.39(2)	Cu2−O8	2.42(2)
Cu1−O4f	2.63(3)	Cu2−O7f	2.46(2)
<Cu1−ϕ>	2.14	<Cu2−ϕ>	2.12
<Cu1−ϕ_{eq}>	1.96	<Cu2−$\phi_{\varepsilon\theta}$>	1.96
<Cu1−ϕ_{ap}>	2.51	<Cu2−ϕ_{ap}>	2.44

a = x+1, y, z; b = x, y−1, z; c = $\bar{x}$+½, y−½, $\bar{z}$+½; d = $\bar{x}$+½, y+½, $\bar{z}$+½; e = x−1, y, z; f = $\bar{x}$+1, y+½, $\bar{z}$+1; g = $\bar{x}$+1, y+½, $\bar{z}$; h = x, y, z−1; i = x, y+1, z; j = $\bar{x}$+2, y−½, $\bar{z}$+1; k = $\bar{x}$+1, y−½, $\bar{z}$+1.

owing to the influence of the twinning. We investigated all available crystals, and collected data for the best. We attribute the uncertainties in the final refinement to the twinning of the crystal, which is probably present on a very fine scale, and to the significant chemical zoning.

Structure description

Chemistry

The EMPA (Table 2) revealed that the crystal used for the crystallography was Fe-rich in the core, where the composition is close to endmember chenevixite, whereas the rim contains more Al than Fe in some of the analysis. Thus, the crystal represents a solid-solution series between chenevixite and luetheite, although it is not clear as to whether the zoning is the result of alteration, corresponds to an overgrowth, or a combination of both.

Formula of chenevixite

Each site in the structure is on a general position, and the $(OH)^-$ groups were readily recognized following a bond-valence analysis done using the parameters given by Brese and O'Keeffe (1991). The structural formula of the crystal is $Cu_2M_2(AsO_4)_2(OH)_4$ where *M* corresponds to Fe^{3+} and Al in varying proportions. This is in good agreement with the formulae given for luetheite and chenevixite by Williams (1977), except that H_2O was not found in the X-ray study. Careful examination of the final difference-Fourier maps did not reveal the presence of any significant electron density that was unaccounted for, and apparently the presence of H_2O in these minerals has not been established by spectroscopic methods.

Cation coordination

Two symmetrically distinct As^{5+} are coordinated by four O atoms in a tetrahedral arrangement, with <As1−O> and <As2−O> bond lengths 1.73 and 1.67 Å, respectively. There are two symmetrically distinct *M* sites, designated *M*1 and *M*2, that are occupied by trivalent cations. Constrained site-occupancy refinement indicates that the *M*1 site contains 0.30(2) Fe and 0.70(2) Al, and the *M*2 site contains 0.43(2) Fe and 0.57(2) Al. Both *M* sites are coordinated by three O atoms and three $(OH)^-$ groups in an octahedral arrangement, with <*M*1−ϕ> and <*M*2−ϕ> bond lengths 1.99 and 2.02 Å, respectively (ϕ: O^{2-}, OH^-).

Two symmetrically distinct Cu^{2+} sites are octahedrally coordinated by four atoms of O and two $(OH)^-$ groups. Both octahedra are strongly distorted, such that there are four short equatorial bonds and two longer apical bonds. The latter are in a *trans* arrangement, a (4+2) distortion consistent with the Jahn-Teller effect associated with a d^9 cation in an octahedral ligand-field. The <Cu1−ϕ> and <Cu2−ϕ> bond lengths are 2.14 and 2.12 Å, respectively, and the <Cu1−ϕ_{eq}> and <Cu2−ϕ_{eq}> bond-lengths are 1.96 Å, typical for $Cu^{2+}\phi_6$ octahedra (Burns and Hawthorne, 1996).

Structure connectivity

In the description and illustrations of the structure that follow, reference is made only to the *B*-centred unit-cell given in Table 1. Projection of the structure onto (010) (Fig. 1) shows that it is composed of a framework of edge and corner-sharing polyhedra.

The structure is best described by making reference to sheets that are parallel to (001) and that are three polyhedra wide. Three views of the

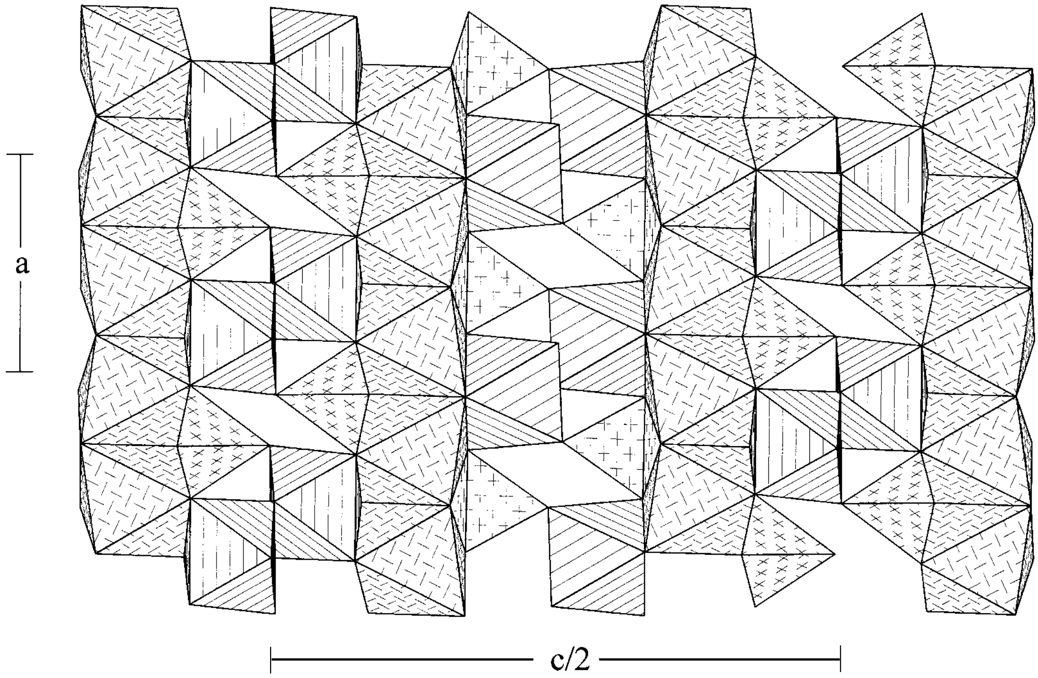

FIG. 1. The structure of chenevixite down [010]. $Cu^{2+}\phi_6$ octahedra are shaded with a herring-bond pattern, $M\phi_6$ octahedra are shaded with parallel lines, and $As\phi_4$ tetrahedra are shaded with crosses.

sheet of polyhedra are presented in Fig. 2. The (4+2)-distorted $Cu^{2+}\phi_6$ octahedra share equatorial edges to form chains that extend along [100]. The $M1\phi_6$ and $M2\phi_6$ octahedra are attached to opposing sides of the chain of edge-sharing $Cu^{2+}\phi_6$ octahedra (Fig. 2c). Each $M\phi_6$ octahedron shares three anions with the chain; one is an equatorial anion that is shared between adjacent $Cu^{2+}\phi_6$ octahedra, and the other two are apical anions of adjacent (4+2)-distorted $Cu^{2+}\phi_6$ octahedra. The resulting chains of octahedra are cross-linked to form the sheet by sharing corners with AsO_4 tetrahedra (Fig. 2b). Each AsO_4 tetrahedron shares three anions within the sheet, and each of the shared anions is an apical anion of a (4+2)-distorted $Cu^{2+}\phi_6$ octahedron, and is also bonded to one $M\phi_6$ octahedron. Each $Cu^{2+}\phi_6$ octahedron contains two O^{2-} and two $(OH)^-$ equatorial anions; only the O^{2-} anions are shared with an AsO_4 tetrahedron. The anions of the AsO_4 tetrahedra (one per tetrahedron) that are not shared within the sheet are shared with $M\phi_6$ octahedra of adjacent sheets (Fig. 1), and the sheets are also connected by the sharing of a single corner between $M\phi_6$ octahedra of adjacent sheets (Fig. 1).

The connectivity between the sheets readily permits twinning on (001). The twin-component scale factor obtained from the refinement was 0.494(4), indicating that the twin components are present in equal proportions. This suggests that the twinning was induced by a phase transition from higher symmetry, possibly orthorhombic, during cooling of the crystals.

Related species

The structures of Cu^{2+} oxysalt minerals are discussed in considerable detail by Eby and Hawthorne (1993). As can be seen in Fig. 1, the structure of chenevixite is based upon a framework of vertex- and edge-sharing polyhedra. Although frameworks are by far the largest class of Cu^{2+} oxysalt structures (Eby and Hawthorne, 1993), the structure of chenevixite is unique amongst Cu^{2+} oxysalts.

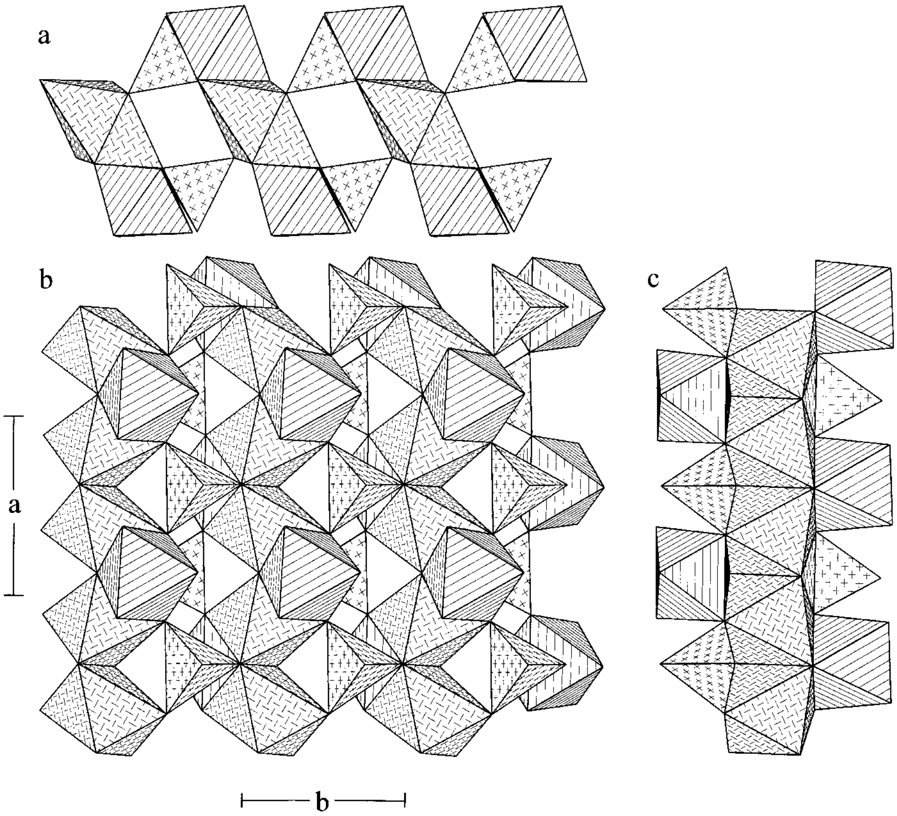

FIG. 2. Sheet of polyhedra from the structure of chenevixite. (a) projected along [001], (b) projected onto (100), (c) projected along [010]. Legend as in Fig. 1.

Acknowledgements

JVS thanks Sidney Williams for the specimen studied. IMS thanks NSF for funding of the electron microprobe. PCB thanks the University of Notre Dame for providing resources for the crystal structures laboratory.

References

Brese, N.E. and O'Keeffe, M. (1991) Bond-valence parameters for solids. *Acta Crystallogr.*, **B47**, 192–7.

Burns, P.C. (1998) CCD area detectors of X-rays applied to the analysis of mineral structures. *Canad. Mineral.,* **36**, 847–853.

Burns, P.C. and Hawthorne, F.C. (1996) Static and dynamic Jahn-Teller effects in Cu^{2+} oxysalts. *Canad. Mineral.,* **34**, 1089–105.

Eby, R.K. and Hawthorne, F.C. (1993) Structural relations in copper oxysalt minerals. I. Structural hierarchy. *Acta Crystallogr.*, **B49**, 28–56.

Herbst-Irmer, R. and Sheldrick, G.M. (1998) Refinement of twinned structures with *SHELXL97*. *Acta Crystallogr.,* **B54**, 443–9.

Ibers, J.A. and Hamilton, W.C., eds. (1974): *International Tables for X-ray Crystallography,* **IV**. The Kynoch Press, Birmingham, U.K.

Jameson, G.B. (1982) On structure refinement using data from a twinned crystal. *Acta Crystallogr.,* **A38**, 817–20.

Williams, S. (1977) Luetheite, $Cu_2Al_2(AsO_4)_2(OH)_2.H_2O$, a new mineral from Arizona, compared with chenevixite. *Mineral. Mag.,* **41**, 27–32.

[*Manuscript received 13 March 1999: revised 29 June 1999*]

Arizona porphyry copper/hydrothermal deposits I. The structure of chenevixite and luetheite. Structure Factor Tables

P. C. Burns[1], J. V. Smith[2] and I. M. Steele[2]

[1] Department of Civil Engineering and Geological Sciences, University of Notre Dame, 156 Fitzpatrick, Notre Dame, IN 46556 USA
[2] Department of Geophysical Sciences, University of Chicago, Chicago, IL 60637 USA

h	k	l	F_{obs}	F_{calc}	Phase	h	k	l	F_{obs}	F_{calc}	Phase
2	0	0	13.32	8.65	180.00	−3	4	1	30.70	27.71	227.65
4	0	0	482.64	447.51	180.00	−1	4	1	126.55	121.25	288.20
2	1	0	291.02	265.30	135.99	1	4	1	30.06	29.29	25.91
4	1	0	16.64	15.63	4.93	3	4	1	111.42	104.40	110.47
6	1	0	143.01	140.39	316.27	5	4	1	21.20	19.27	180.21
0	2	0	257.10	239.72	100.91	−3	5	1	93.73	100.95	248.31
2	2	0	12.70	16.34	276.25	−1	5	1	9.39	9.87	75.57
4	2	0	145.54	139.61	287.43	1	5	1	113.57	119.04	68.82
6	2	0	17.84	18.34	112.61	3	5	1	6.11	6.68	306.58
2	3	0	248.24	228.84	246.21	−1	6	1	80.87	76.09	31.35
4	3	0	21.89	21.49	121.00	1	6	1	30.00	29.80	257.87
6	3	0	123.70	115.86	63.53	−4	0	2	56.95	53.00	0.00
0	4	0	176.15	158.58	197.38	−2	0	2	7.59	6.46	180.00
2	4	0	0.00	6.59	55.10	0	0	2	6.55	7.81	0.00
4	4	0	130.50	125.28	21.04	2	0	2	38.35	41.23	180.00
2	5	0	73.93	78.77	352.68	6	0	2	19.49	40.40	0.00
4	5	0	17.70	17.50	179.97	−6	1	2	20.00	14.62	356.73
0	6	0	31.60	24.78	72.20	−4	1	2	29.33	31.92	129.43
−3	0	1	9.84	8.06	180.00	−2	1	2	26.12	26.11	60.88
−1	0	1	8.72	12.88	180.00	0	1	2	50.70	53.30	312.52
1	0	1	5.67	5.85	180.00	2	1	2	24.28	37.29	209.97
3	0	1	7.68	8.32	180.00	4	1	2	19.33	19.53	124.50
5	0	1	23.31	5.68	0.00	6	1	2	41.04	36.22	308.31
−5	1	1	66.66	58.39	128.50	−6	2	2	41.46	41.03	100.09
−3	1	1	134.87	136.29	48.72	−4	2	2	60.37	61.08	34.49
−1	1	1	69.80	79.59	312.73	−2	2	2	102.80	101.98	284.38
1	1	1	159.29	186.76	232.53	0	2	2	72.01	65.63	177.44
3	1	1	41.59	42.22	139.09	2	2	2	96.27	92.28	110.66
5	1	1	97.15	92.41	52.90	4	2	2	48.17	51.54	324.93
−5	2	1	44.42	42.07	348.03	6	2	2	32.26	31.21	295.18
−3	2	1	89.10	89.49	275.16	−6	3	2	122.84	114.17	341.69
−1	2	1	81.00	80.74	170.56	−4	3	2	52.82	48.88	226.15
1	2	1	97.77	97.14	93.80	−2	3	2	250.76	223.67	152.48
3	2	1	81.50	78.40	355.62	0	3	2	77.96	74.85	55.79
5	2	1	55.04	52.12	279.23	2	3	2	251.85	229.33	323.15
−5	3	1	27.79	30.57	217.32	4	3	2	53.11	42.45	236.83
−3	3	1	10.46	13.55	208.81	6	3	2	120.33	110.66	133.13
−1	3	1	35.80	37.51	30.38	−4	4	2	92.59	80.23	117.74
1	3	1	15.04	15.81	58.12	−2	4	2	13.17	22.03	344.89
3	3	1	32.35	29.99	201.31	0	4	2	108.64	99.14	287.00
5	3	1	14.80	9.83	196.98	2	4	2	18.31	18.53	194.19
−5	4	1	86.14	75.96	105.01	4	4	2	78.51	68.98	92.30

h	k	l	F_{obs}	F_{calc}	Phase	h	k	l	F_{obs}	F_{calc}	Phase
−4	5	2	62.57	64.74	348.61	−2	2	4	97.30	93.53	191.79
−2	5	2	22.90	23.87	295.57	0	2	4	212.70	195.76	278.76
0	5	2	93.19	93.96	172.16	2	2	4	122.03	114.86	27.77
2	5	2	20.41	12.61	53.48	4	2	4	145.22	131.51	102.11
4	5	2	76.10	69.49	352.18	6	2	4	49.87	62.41	211.64
−2	6	2	71.24	84.34	102.30	−6	3	4	61.66	61.34	70.00
0	6	2	56.90	60.79	47.43	−4	3	4	125.90	126.21	131.29
−5	0	3	33.72	35.01	180.00	−2	3	4	145.36	135.76	244.49
−3	0	3	18.76	18.37	0.00	0	3	4	186.43	170.91	317.02
−1	0	3	40.75	45.11	0.00	2	3	4	143.99	138.51	52.62
1	0	3	1.97	1.82	0.00	4	3	4	135.97	129.68	146.84
3	0	3	33.63	32.63	180.00	−4	4	4	26.74	28.98	196.35
5	0	3	1.18	0.80	0.00	−2	4	4	109.45	103.33	294.57
−5	1	3	6.74	6.11	257.39	0	4	4	53.98	58.48	6.87
−3	1	3	135.06	132.81	319.16	2	4	4	123.39	111.41	125.77
−1	1	3	16.67	18.67	248.38	4	4	4	52.65	48.02	185.47
1	1	3	167.15	183.01	144.84	−4	5	4	48.48	56.15	227.11
3	1	3	26.83	29.12	68.16	−2	5	4	99.16	97.42	340.13
5	1	3	107.12	100.84	330.31	0	5	4	72.89	62.05	64.55
−5	2	3	124.43	122.72	280.71	2	5	4	88.74	92.65	154.60
−3	2	3	18.81	19.47	136.47	−2	6	4	51.50	54.46	23.35
−1	2	3	191.32	191.88	101.92	0	6	4	111.59	110.70	117.68
1	2	3	25.43	26.42	344.32	−5	0	5	12.04	12.15	0.00
3	2	3	167.57	167.72	279.86	−3	0	5	51.00	87.25	0.00
5	2	3	24.21	22.49	186.17	−1	0	5	6.74	6.52	180.00
−5	3	3	17.38	19.62	119.42	1	0	5	120.40	134.79	180.00
−3	3	3	90.10	88.51	69.62	3	0	5	20.64	21.08	180.00
−1	3	3	34.47	33.91	338.63	5	0	5	86.04	86.41	0.00
1	3	3	94.48	98.25	257.32	−5	1	5	95.04	93.63	321.07
3	3	3	45.87	45.16	171.46	−3	1	5	98.43	105.09	56.52
5	3	3	69.25	55.92	86.95	−1	1	5	165.63	180.45	136.15
−5	4	3	31.06	28.36	195.09	1	1	5	124.63	132.91	224.89
−3	4	3	46.68	42.82	292.64	3	1	5	139.61	142.27	315.13
−1	4	3	56.41	50.84	1.61	5	1	5	76.25	74.49	38.44
1	4	3	76.67	70.91	110.65	−5	2	5	30.15	27.71	11.83
3	4	3	45.22	45.64	166.83	−3	2	5	98.34	97.46	93.14
5	4	3	77.34	51.89	290.85	−1	2	5	55.05	50.78	180.09
−3	5	3	12.14	26.65	242.49	1	2	5	116.87	121.98	277.66
−1	5	3	12.01	17.21	37.28	3	2	5	40.33	41.68	349.09
1	5	3	27.29	29.12	72.47	5	2	5	101.31	89.76	99.54
3	5	3	17.91	23.33	237.77	−5	3	5	57.14	60.48	61.31
−1	6	3	44.20	41.56	317.66	−3	3	5	39.68	37.43	321.54
1	6	3	42.75	38.12	218.21	−1	3	5	111.99	112.44	236.87
−6	0	4	50.47	33.88	180.00	1	3	5	41.04	42.08	164.87
−4	0	4	55.58	40.37	0.00	3	3	5	106.74	97.41	57.78
−2	0	4	0.00	23.37	0.00	5	3	5	33.59	24.92	7.10
0	0	4	74.81	86.51	180.00	−5	4	5	31.89	28.46	115.87
2	0	4	12.06	12.77	0.00	−3	4	5	28.32	25.38	156.15
4	0	4	56.82	49.82	0.00	−1	4	5	34.51	35.43	297.95
6	0	4	20.49	11.73	180.00	1	4	5	17.24	23.09	313.85
−6	1	4	18.77	25.50	334.47	3	4	5	42.46	27.97	122.66
−4	1	4	31.46	35.79	271.25	5	4	5	22.20	10.50	113.96
−2	1	4	28.19	25.72	178.89	−3	5	5	84.92	85.36	241.74
0	1	4	60.27	49.92	48.58	−1	5	5	8.49	8.19	272.50
2	1	4	55.86	52.72	311.34	1	5	5	98.26	94.99	63.90
4	1	4	42.63	39.36	189.05	3	5	5	9.22	8.64	107.68
6	1	4	29.01	50.92	127.87	−1	6	5	39.21	26.52	38.44
−6	2	4	41.89	48.78	346.75	1	6	5	25.42	19.89	55.52
−4	2	4	131.31	125.60	96.80	−6	0	6	189.31	189.06	180.00

h	k	l	F_{obs}	F_{calc}	Phase	h	k	l	F_{obs}	F_{calc}	Phase
−4	0	6	22.41	29.45	180.00	3	3	7	34.94	30.01	155.69
−2	0	6	421.75	381.88	0.00	5	3	7	62.38	36.35	253.24
0	0	6	12.73	8.70	0.00	−5	4	7	28.96	36.71	219.78
2	0	6	388.91	358.73	180.00	−3	4	7	93.21	94.20	288.48
4	0	6	1.77	8.62	180.00	−1	4	7	63.66	62.46	23.32
6	0	6	180.12	171.54	0.00	1	4	7	105.76	103.01	107.29
−6	1	6	37.82	45.66	57.43	3	4	7	64.50	60.25	193.09
−4	1	6	202.68	189.75	318.63	5	4	7	78.47	65.16	284.57
−2	1	6	124.90	114.08	239.14	−3	5	7	23.24	23.58	67.71
0	1	6	367.33	339.78	139.62	−1	5	7	134.82	130.53	72.57
2	1	6	115.19	107.39	46.05	1	5	7	12.24	11.84	246.86
4	1	6	229.09	207.41	321.62	3	5	7	114.12	110.12	254.68
6	1	6	43.85	47.13	200.25	−1	6	7	33.18	38.09	273.16
−6	2	6	69.91	71.17	276.51	1	6	7	80.36	78.24	207.96
−4	2	6	56.98	49.58	353.08	−6	0	8	64.07	38.19	0.00
−2	2	6	138.48	137.46	96.13	−4	0	8	35.20	27.89	0.00
0	2	6	133.85	139.49	192.88	−2	0	8	24.76	25.87	180.00
2	2	6	136.12	127.14	279.45	0	0	8	63.02	53.68	180.00
4	2	6	38.68	37.25	34.33	2	0	8	6.82	15.67	180.00
6	2	6	57.50	59.21	104.63	4	0	8	50.15	46.54	0.00
−6	3	6	23.79	31.44	195.46	6	0	8	50.86	35.23	0.00
−4	3	6	133.74	123.92	60.94	−6	1	8	0.00	21.24	179.84
−2	3	6	65.20	58.69	358.05	−4	1	8	88.69	86.72	199.06
0	3	6	171.84	168.67	239.90	−2	1	8	110.64	115.92	325.87
2	3	6	62.96	60.26	155.54	0	1	8	129.24	123.06	41.30
4	3	6	119.74	113.73	62.82	2	1	8	116.80	123.17	135.78
−4	4	6	24.90	35.24	312.07	4	1	8	82.75	85.22	251.81
−2	4	6	195.92	194.87	198.58	6	1	8	15.60	17.06	303.42
0	4	6	43.90	40.50	125.12	−6	2	8	39.19	31.73	94.02
2	4	6	191.56	191.73	23.25	−4	2	8	21.21	25.63	233.05
4	4	6	48.07	43.68	276.43	−2	2	8	20.32	23.17	247.93
−4	5	6	52.05	62.79	154.38	0	2	8	40.80	43.55	97.69
−2	5	6	67.61	58.61	63.61	2	2	8	26.60	31.52	336.47
0	5	6	75.28	79.34	336.97	4	2	8	7.01	18.77	290.67
2	5	6	81.41	64.61	231.98	6	2	8	65.78	31.62	115.73
4	5	6	76.42	56.90	163.45	−4	3	8	94.27	85.26	170.64
0	6	6	74.19	65.50	213.20	−2	3	8	15.16	13.18	106.11
−5	0	7	94.36	88.47	0.00	0	3	8	122.82	109.78	335.06
−3	0	7	11.39	11.46	180.00	2	3	8	0.00	8.60	262.44
−1	0	7	162.62	159.93	180.00	4	3	8	81.99	69.77	133.70
1	0	7	0.17	0.19	0.00	−4	4	8	19.21	26.91	28.75
3	0	7	103.93	112.32	0.00	−2	4	8	11.70	9.26	218.15
5	0	7	11.41	10.64	0.00	0	4	8	37.84	47.79	219.51
−5	1	7	72.53	63.41	55.94	2	4	8	35.82	36.42	24.60
−3	1	7	50.12	44.61	139.50	4	4	8	38.33	30.81	34.11
−1	1	7	113.15	113.06	235.03	−2	5	8	24.60	33.58	159.17
1	1	7	62.49	70.14	316.42	0	5	8	67.37	60.13	234.60
3	1	7	89.41	97.86	42.52	2	5	8	35.45	29.21	335.80
5	1	7	51.62	46.62	134.39	4	5	8	61.98	51.22	67.22
−5	2	7	46.28	43.80	243.92	0	6	8	71.91	72.45	302.44
−3	2	7	84.38	76.98	189.48	−5	0	9	25.00	17.71	0.00
−1	2	7	65.19	67.09	78.14	−3	0	9	28.36	31.00	180.00
1	2	7	88.97	93.73	11.98	−1	0	9	29.39	23.93	180.00
3	2	7	38.29	38.03	277.40	1	0	9	41.93	48.89	0.00
5	2	7	61.09	51.20	188.07	3	0	9	26.93	28.37	0.00
−5	3	7	23.22	25.68	176.59	5	0	9	44.23	28.25	180.00
−3	3	7	58.58	55.51	267.67	−5	1	9	52.21	46.60	320.37
−1	3	7	32.77	34.45	355.35	−3	1	9	10.30	8.97	150.23
1	3	7	68.02	68.70	79.88	−1	1	9	71.80	73.08	152.73

h	k	l	F_{obs}	F_{calc}	Phase	h	k	l	F_{obs}	F_{calc}	Phase
1	1	9	19.29	18.47	155.32	2	5	10	42.05	30.37	272.26
3	1	9	53.96	56.57	337.72	4	5	10	75.95	57.91	322.23
5	1	9	16.37	14.83	328.03	0	6	10	48.55	59.75	200.21
−5	2	9	44.65	44.59	161.88	−5	0	11	87.10	89.85	0.00
−3	2	9	144.94	144.16	101.26	−3	0	11	21.47	20.95	180.00
−1	2	9	70.33	72.90	0.56	−1	0	11	125.18	123.49	180.00
1	2	9	179.03	180.62	283.58	1	0	11	3.92	4.21	180.00
3	2	9	65.25	66.67	192.84	3	0	11	93.72	97.03	0.00
5	2	9	99.31	98.16	110.42	5	0	11	13.13	10.60	0.00
−5	3	9	20.74	25.15	34.26	−5	1	11	51.46	52.76	53.86
−3	3	9	92.76	96.16	333.04	−3	1	11	128.35	130.25	140.78
−1	3	9	14.77	15.52	220.27	−1	1	11	89.84	86.76	223.69
1	3	9	112.44	108.33	150.97	1	1	11	150.38	151.76	321.18
3	3	9	9.88	10.06	108.72	3	1	11	68.83	71.59	31.56
5	3	9	75.23	70.59	326.12	5	1	11	87.07	84.78	142.02
−5	4	9	56.36	71.79	284.02	−5	2	11	70.53	77.00	97.10
−3	4	9	36.91	35.28	349.67	−3	2	11	31.51	30.15	343.97
−1	4	9	114.42	111.49	106.68	−1	2	11	131.00	128.61	273.90
1	4	9	55.19	54.51	156.13	1	2	11	24.55	23.63	197.18
3	4	9	117.40	94.43	289.12	3	2	11	111.42	111.76	90.85
5	4	9	60.90	47.93	329.22	5	2	11	15.67	13.77	57.13
−3	5	9	16.05	41.46	69.98	−5	3	11	52.12	59.60	326.88
−1	5	9	17.12	17.67	30.63	−3	3	11	66.14	66.04	236.93
1	5	9	62.35	58.84	248.15	−1	3	11	91.13	93.10	154.29
3	5	9	27.16	18.02	236.92	1	3	11	73.80	72.63	54.67
1	6	9	28.67	26.10	136.54	3	3	11	82.95	85.83	337.82
−6	0	10	63.01	67.76	0.00	5	3	11	64.72	45.18	243.87
−4	0	10	20.70	2.59	0.00	−5	4	11	21.64	32.14	180.85
−2	0	10	153.37	129.76	180.00	−3	4	11	31.18	43.07	108.18
0	0	10	7.36	3.58	0.00	−1	4	11	52.73	48.00	0.08
2	0	10	136.44	127.22	0.00	1	4	11	56.25	52.37	287.12
4	0	10	0.00	1.95	180.00	3	4	11	57.87	40.05	188.26
6	0	10	77.01	73.01	180.00	5	4	11	68.31	32.15	107.08
−6	1	10	27.88	35.09	268.77	−3	5	11	10.61	13.64	294.05
−4	1	10	177.06	164.88	146.02	−1	5	11	42.49	46.30	56.95
−2	1	10	91.98	93.93	62.37	1	5	11	28.39	22.82	107.55
0	1	10	276.62	265.87	327.85	3	5	11	60.19	39.74	237.23
2	1	10	89.11	88.36	212.53	−6	0	12	9.20	8.89	180.00
4	1	10	177.06	171.83	147.67	−4	0	12	86.53	79.04	0.00
6	1	10	36.28	38.57	11.24	−2	0	12	3.85	3.77	180.00
−6	2	10	132.75	141.56	101.21	0	0	12	57.15	46.10	180.00
−4	2	10	41.72	41.73	186.42	2	0	12	9.91	28.87	0.00
−2	2	10	278.50	271.34	279.53	4	0	12	81.50	79.36	0.00
0	2	10	42.80	41.08	31.52	6	0	12	30.08	30.04	180.00
2	2	10	293.78	274.89	97.08	−6	1	12	77.37	83.84	320.66
4	2	10	27.87	28.02	217.68	−4	1	12	62.34	58.76	244.65
6	2	10	147.32	148.33	274.48	−2	1	12	179.30	177.03	139.88
−4	3	10	107.70	105.38	247.99	0	1	12	59.95	50.40	35.45
−2	3	10	72.02	67.89	324.46	2	1	12	164.27	162.34	321.57
0	3	10	160.43	155.31	61.97	4	1	12	41.35	44.55	195.19
2	3	10	86.23	77.50	156.54	6	1	12	78.18	67.13	147.11
4	3	10	119.16	112.40	238.93	−6	2	12	59.75	51.73	209.56
−4	4	10	47.46	52.12	264.69	−4	2	12	25.90	26.58	74.90
−2	4	10	82.84	84.00	38.04	−2	2	12	95.11	91.05	20.45
0	4	10	54.92	49.40	102.46	0	2	12	27.86	18.61	286.14
2	4	10	92.01	89.01	212.96	2	2	12	96.68	93.69	186.36
4	4	10	53.53	39.63	308.79	4	2	12	14.81	9.00	81.91
−2	5	10	18.18	35.83	71.57	−4	3	12	41.89	39.45	345.78
0	5	10	65.62	68.88	145.05	−2	3	12	83.66	87.60	228.73

h	k	l	F_{obs}	F_{calc}	Phase	h	k	l	F_{obs}	F_{calc}	Phase
0	3	12	38.61	36.19	134.05	0	2	14	35.52	37.96	161.47
2	3	12	81.24	83.02	57.18	2	2	14	44.29	39.43	249.45
4	3	12	52.41	39.18	288.12	4	2	14	45.07	32.96	37.81
−4	4	12	138.39	143.52	195.35	−4	3	14	14.75	27.35	56.48
−2	4	12	89.21	87.21	127.75	−2	3	14	44.62	44.86	137.26
0	4	12	204.41	201.00	18.25	0	3	14	42.14	49.66	240.20
2	4	12	98.00	84.76	295.29	2	3	14	47.54	52.92	344.30
4	4	12	143.80	136.55	198.43	4	3	14	39.32	30.83	62.04
−2	5	12	70.59	75.51	327.46	−4	4	14	53.72	54.39	84.25
0	5	12	141.10	131.85	251.40	−2	4	14	48.86	55.06	201.67
2	5	12	83.51	72.88	156.77	0	4	14	67.15	65.18	287.77
0	6	12	14.73	29.57	120.11	2	4	14	52.96	50.00	13.85
−5	0	13	4.85	4.65	180.00	4	4	14	83.93	55.33	126.16
−3	0	13	168.57	164.51	180.00	−2	5	14	103.22	103.16	245.80
−1	0	13	8.43	9.60	0.00	0	5	14	49.87	51.11	325.01
1	0	13	173.15	192.29	0.00	2	5	14	116.54	107.04	73.79
3	0	13	3.12	3.57	180.00	−5	0	15	60.11	60.53	180.00
5	0	13	125.49	128.07	180.00	−3	0	15	16.24	14.62	180.00
−5	1	13	91.89	91.55	143.62	−1	0	15	97.02	103.00	0.00
−3	1	13	45.00	41.90	243.37	1	0	15	15.71	15.36	0.00
−1	1	13	164.03	146.72	321.34	3	0	15	90.10	97.67	180.00
1	1	13	46.96	49.14	45.27	5	0	15	7.91	6.25	180.00
3	1	13	102.33	113.28	138.15	−5	1	15	26.29	20.78	81.08
5	1	13	39.69	37.85	211.10	−3	1	15	40.20	36.28	307.18
−5	2	13	44.22	39.68	210.86	−1	1	15	45.86	43.17	248.41
−3	2	13	26.45	21.78	343.68	1	1	15	61.81	64.61	143.01
−1	2	13	46.32	48.23	39.11	3	1	15	29.62	33.69	79.09
1	2	13	22.65	22.57	156.01	5	1	15	56.20	50.65	327.67
3	2	13	21.95	22.63	222.21	−5	2	15	36.61	39.01	96.90
5	2	13	28.08	18.15	307.55	−3	2	15	64.27	71.36	12.03
−5	3	13	40.34	45.04	267.50	−1	2	15	57.05	60.01	289.85
−3	3	13	20.99	20.27	343.06	1	2	15	79.51	81.11	197.91
−1	3	13	70.53	63.45	77.57	3	2	15	36.67	40.27	130.76
1	3	13	12.04	11.11	161.52	5	2	15	45.48	46.93	18.56
3	3	13	63.49	58.16	245.14	−5	3	15	92.92	94.45	325.90
5	3	13	7.26	3.95	233.46	−3	3	15	19.89	20.69	63.58
−5	4	13	22.98	35.29	314.17	−1	3	15	132.33	138.43	145.02
−3	4	13	75.20	83.17	31.24	1	3	15	22.46	22.81	234.27
−1	4	13	34.97	34.86	129.86	3	3	15	118.77	112.90	323.55
1	4	13	98.55	93.93	209.45	5	3	15	22.00	16.76	41.15
3	4	13	22.10	19.24	295.33	−3	4	15	54.61	66.17	101.20
−3	5	13	68.25	79.61	70.16	−1	4	15	51.31	53.69	181.87
−1	5	13	18.60	20.90	229.93	1	4	15	72.73	71.42	278.10
1	5	13	93.58	81.48	247.37	3	4	15	64.55	55.28	2.65
3	5	13	19.26	15.64	22.53	−1	5	15	50.20	59.54	262.45
−4	0	14	23.66	15.32	180.00	1	5	15	10.03	8.06	259.27
−2	0	14	65.30	56.11	0.00	3	5	15	71.98	54.41	79.75
2	0	14	80.82	83.06	180.00	−4	0	16	138.17	139.60	180.00
4	0	14	16.59	21.10	0.00	−2	0	16	33.66	17.30	180.00
6	0	14	50.85	27.37	0.00	0	0	16	240.03	223.97	0.00
−6	1	14	101.61	97.75	196.64	2	0	16	8.91	10.15	180.00
−4	1	14	0.00	8.27	271.84	4	0	16	156.06	152.32	180.00
−2	1	14	190.90	182.96	35.93	6	0	16	41.70	19.93	0.00
0	1	14	26.94	31.70	114.11	−6	1	16	137.86	145.03	140.31
2	1	14	178.80	179.97	231.67	−4	1	16	24.63	18.22	104.70
4	1	14	29.38	15.04	282.08	−2	1	16	304.56	285.69	320.60
6	1	14	93.99	84.96	61.17	0	1	16	32.63	26.90	255.28
−4	2	14	44.29	45.94	320.40	2	1	16	282.28	275.29	143.01
−2	2	14	13.85	18.27	72.23	4	1	16	27.95	24.30	51.47

h	k	l	F_{obs}	F_{calc}	Phase	h	k	l	F_{obs}	F_{calc}	Phase
6	1	16	159.23	141.96	324.44	4	1	18	20.81	11.27	340.26
−4	2	16	227.64	232.00	284.33	−4	2	18	97.62	96.79	19.62
−2	2	16	29.14	32.70	244.47	−2	2	18	35.04	30.73	61.97
0	2	16	336.07	333.70	102.13	0	2	18	149.60	141.54	185.08
2	2	16	28.15	33.00	40.44	2	2	18	41.41	37.89	243.37
4	2	16	234.44	230.75	280.55	4	2	18	91.14	88.93	343.79
−4	3	16	26.11	33.89	335.99	−4	3	18	50.71	56.19	236.56
−2	3	16	147.22	144.11	58.62	−2	3	18	25.56	19.15	184.46
0	3	16	38.10	44.61	186.52	0	3	18	74.99	82.41	65.83
2	3	16	152.07	149.89	242.13	2	3	18	22.46	17.06	300.74
4	3	16	43.40	34.60	28.55	4	3	18	57.51	50.62	245.58
−4	4	16	37.09	44.09	53.21	−4	4	18	68.17	75.23	123.71
−2	4	16	15.87	23.51	52.73	−2	4	18	72.49	78.83	7.27
0	4	16	49.65	52.53	226.37	0	4	18	101.30	94.54	292.17
2	4	16	15.30	8.98	240.69	2	4	18	77.49	80.44	189.15
4	4	16	63.58	37.50	41.75	0	5	18	74.40	72.58	168.51
−2	5	16	49.37	60.61	177.35	2	5	18	109.84	99.91	70.18
0	5	16	41.11	26.91	46.12	−5	0	19	122.13	131.53	180.00
2	5	16	88.35	65.82	357.19	−3	0	19	15.67	17.32	0.00
−5	0	17	8.17	8.86	180.00	−1	0	19	210.28	209.28	0.00
−3	0	17	88.50	92.01	180.00	1	0	19	3.15	3.16	180.00
−1	0	17	9.83	10.77	0.00	3	0	19	162.95	183.12	180.00
1	0	17	90.42	88.73	0.00	5	0	19	6.50	6.59	180.00
3	0	17	12.41	13.36	180.00	−5	1	19	16.74	19.58	256.91
5	0	17	50.43	40.67	180.00	−3	1	19	97.57	102.58	321.67
−5	1	17	37.82	38.06	132.64	−1	1	19	28.45	27.84	65.96
−3	1	17	51.42	53.10	220.93	1	1	19	109.39	113.03	140.06
−1	1	17	42.12	42.99	309.48	3	1	19	12.37	13.91	247.20
1	1	17	65.80	67.77	37.13	5	1	19	73.89	70.85	320.89
3	1	17	30.24	34.54	121.45	−5	2	19	26.18	21.99	283.15
5	1	17	36.66	38.05	214.22	−3	2	19	30.72	32.15	158.19
−5	2	17	37.51	45.98	5.27	−1	2	19	37.97	31.69	120.87
−3	2	17	45.04	45.38	276.35	1	2	19	40.97	41.59	355.52
−1	2	17	82.22	79.63	193.34	3	2	19	29.58	30.79	313.55
1	2	17	49.93	50.52	96.28	5	2	19	38.61	24.16	182.99
3	2	17	64.98	70.38	16.00	−3	3	19	37.35	42.96	78.43
5	2	17	33.13	27.17	287.04	−1	3	19	26.68	28.23	312.28
−3	3	17	114.32	123.58	147.98	1	3	19	52.62	49.09	264.58
−1	3	17	21.81	22.96	28.08	3	3	19	57.62	41.63	146.28
1	3	17	149.87	148.31	327.08	5	3	19	59.46	36.94	89.93
3	3	17	15.42	14.65	222.57	−3	4	19	19.61	21.88	250.19
5	3	17	121.38	100.95	145.67	−1	4	19	89.97	93.68	209.63
−3	4	17	25.43	28.93	6.53	1	4	19	34.47	31.82	89.55
−1	4	17	66.57	71.79	291.71	3	4	19	78.93	78.19	32.48
1	4	17	41.21	36.97	191.04	−1	5	19	5.12	8.24	97.70
3	4	17	83.76	64.55	117.83	1	5	19	80.48	15.42	55.44
−1	5	17	2.74	22.43	92.02	−4	0	20	94.55	87.09	0.00
1	5	17	40.44	26.63	95.42	−2	0	20	0.00	11.38	0.00
−4	0	18	19.70	15.84	0.00	0	0	20	178.80	145.28	180.00
−2	0	18	143.79	116.16	180.00	2	0	20	0.40	19.64	0.00
0	0	18	19.30	2.44	0.00	4	0	20	104.29	101.82	0.00
2	0	18	108.93	114.17	0.00	6	0	20	25.39	15.88	180.00
4	0	18	29.86	35.97	180.00	−4	1	20	84.21	79.81	38.87
6	0	18	64.43	47.20	180.00	−2	1	20	24.96	21.46	100.75
−6	1	18	47.75	48.97	256.22	0	1	20	107.24	106.84	232.35
−4	1	18	1.97	16.64	109.65	2	1	20	26.07	30.89	292.89
−2	1	18	77.14	67.65	54.15	4	1	20	76.49	81.50	59.83
0	1	18	9.61	6.13	224.95	−4	2	20	43.50	38.43	121.30
2	1	18	70.48	71.35	211.80	−2	2	20	83.47	83.38	178.48

h	k	l	F_{obs}	F_{calc}	Phase
0	2	20	71.92	68.96	279.34
2	2	20	85.53	92.77	13.52
4	2	20	55.29	55.19	92.99
−4	3	20	27.64	26.38	106.11
−2	3	20	78.85	78.46	234.25
0	3	20	23.30	22.10	331.04
2	3	20	85.91	84.02	52.30
4	3	20	43.98	23.54	195.65
−2	4	20	73.29	76.65	277.17
0	4	20	84.69	81.45	12.88
2	4	20	83.24	81.99	106.92
0	5	20	121.43	123.34	68.41
−5	0	21	3.41	3.26	0.00
−3	0	21	111.30	115.23	0.00
−1	0	21	1.00	0.95	0.00
1	0	21	163.76	150.84	180.00
3	0	21	6.73	7.13	180.00
5	0	21	117.42	113.68	0.00
−5	1	21	50.90	64.76	319.67
−3	1	21	29.52	33.51	239.21
−1	1	21	101.93	106.50	138.78
1	1	21	40.41	40.18	91.90
3	1	21	93.90	98.68	317.97
5	1	21	31.15	30.76	291.30
−3	2	21	36.90	38.57	98.35
−1	2	21	26.41	26.90	193.80
1	2	21	52.33	50.05	282.88
3	2	21	20.31	20.27	347.70
5	2	21	46.52	37.31	111.78
−3	3	21	75.24	85.99	140.63
−1	3	21	40.70	43.46	215.38
1	3	21	92.73	98.88	321.93
3	3	21	40.00	44.78	34.05
−3	4	21	49.89	57.49	199.10
−1	4	21	29.65	35.17	280.37
1	4	21	74.14	68.43	18.23
3	4	21	37.33	33.76	90.17
−4	0	22	0.00	26.86	180.00
−2	0	22	145.85	139.54	0.00
0	0	22	23.29	14.71	0.00
2	0	22	133.03	136.95	180.00
4	0	22	8.26	8.53	0.00
−4	1	22	163.34	143.81	317.35
−2	1	22	7.79	6.53	275.17
0	1	22	207.10	200.03	136.13
2	1	22	0.00	16.77	57.59
4	1	22	139.06	145.21	316.59
−4	2	22	8.86	24.53	250.06
−2	2	22	221.65	217.90	99.13
0	2	22	22.98	20.02	60.66
2	2	22	193.15	213.14	281.94
4	2	22	19.74	14.92	185.84
−4	3	22	101.68	112.52	57.14
−2	3	22	19.62	27.35	1.07
0	3	22	145.06	147.07	238.09
2	3	22	31.17	30.94	153.97
4	3	22	95.48	108.54	60.44
−2	4	22	21.89	19.77	180.19
0	4	22	37.72	30.97	82.18
2	4	22	21.83	17.72	13.37
−3	0	23	20.79	14.68	180.00
−1	0	23	45.91	29.28	0.00
1	0	23	16.24	14.63	0.00
3	0	23	37.15	17.11	180.00
−5	1	23	19.33	16.21	225.90
−3	1	23	32.06	31.43	169.56
−1	1	23	31.87	28.59	45.91
1	1	23	44.35	41.34	348.13
3	1	23	25.13	27.12	248.43
5	1	23	48.64	29.35	166.35
−3	2	23	43.64	46.59	205.48
−1	2	23	54.30	55.84	281.27
1	2	23	55.33	56.40	18.81
3	2	23	47.70	51.00	88.94
5	2	23	39.55	41.45	190.04
−3	3	23	16.90	16.68	294.39
−1	3	23	138.64	139.70	328.89
1	3	23	10.35	10.68	80.64
3	3	23	115.25	119.02	148.20
−1	4	23	12.52	15.82	150.29
1	4	23	66.22	66.93	113.59
−4	0	24	56.68	53.06	180.00
−2	0	24	30.42	41.43	180.00
0	0	24	103.03	87.84	0.00
2	0	24	9.39	11.36	0.00
4	0	24	39.21	44.12	180.00
−4	1	24	83.15	77.37	70.39
−2	1	24	13.41	18.33	118.89
0	1	24	110.45	104.84	234.32
2	1	24	21.54	18.72	287.89
4	1	24	74.85	74.48	31.78
−4	2	24	12.50	15.98	88.60
−2	2	24	3.39	6.56	357.89
0	2	24	11.01	15.59	261.30
2	2	24	0.00	28.82	261.37
4	2	24	44.86	20.36	78.94
−4	3	24	17.36	37.94	267.84
−2	3	24	19.95	22.18	78.22
0	3	24	23.55	27.77	102.58
2	3	24	18.68	18.41	244.00
−2	4	24	25.16	26.62	285.80
0	4	24	33.23	42.97	204.80
2	4	24	37.46	26.42	73.38
−5	0	25	20.82	19.24	0.00
−3	0	25	122.48	138.48	0.00
−1	0	25	6.89	6.46	180.00
1	0	25	149.91	152.55	180.00
3	0	25	4.80	6.00	180.00
−3	1	25	22.02	23.29	192.19
−1	1	25	38.87	39.23	134.80
1	1	25	22.93	23.64	26.38
3	1	25	38.51	35.94	324.11
5	1	25	31.46	16.23	215.79
−3	2	25	8.07	10.37	248.12
−1	2	25	54.72	47.76	355.17
1	2	25	18.97	19.43	69.72
3	2	25	41.88	40.52	177.15
−3	3	25	37.37	49.92	315.67

h	k	l	F_{obs}	F_{calc}	Phase	h	k	l	F_{obs}	F_{calc}	Phase
−1	3	25	37.07	36.45	259.98	3	0	29	17.88	16.08	180.00
1	3	25	60.98	62.23	141.99	−3	1	29	9.21	17.58	30.11
3	3	25	33.90	30.37	105.16	−1	1	29	71.55	61.65	327.07
−1	4	25	47.55	56.43	111.59	1	1	29	24.50	21.79	227.26
1	4	25	59.50	61.75	28.67	3	1	29	51.50	54.91	142.51
−2	0	26	180.89	144.98	180.00	−3	2	29	75.40	92.95	289.67
2	0	26	129.41	140.78	0.00	−1	2	29	15.37	18.73	43.01
4	0	26	12.42	5.28	180.00	1	2	29	101.74	102.97	108.02
−4	1	26	95.12	104.91	144.92	3	2	29	6.86	7.39	199.89
−2	1	26	48.22	48.92	236.39	−1	3	29	35.18	38.98	63.80
0	1	26	148.00	149.38	320.87	1	3	29	56.93	70.87	154.33
2	1	26	49.93	52.99	67.29	0	0	30	11.32	16.86	0.00
4	1	26	117.35	117.56	137.35	2	0	30	10.06	3.24	180.00
−4	2	26	44.56	43.12	171.44	4	0	30	0.28	1.44	0.00
−2	2	26	80.41	84.13	285.67	−4	1	30	19.41	10.66	5.39
0	2	26	47.08	53.83	8.34	−2	1	30	42.98	46.14	264.99
2	2	26	79.64	86.43	104.84	0	1	30	23.41	26.44	161.95
4	2	26	48.93	40.95	198.79	2	1	30	38.21	33.83	52.09
−2	3	26	35.01	27.65	165.12	−2	2	30	11.82	14.57	24.76
0	3	26	92.67	99.44	67.62	0	2	30	49.57	50.17	178.17
2	3	26	39.83	30.02	317.34	2	2	30	17.90	15.77	206.33
0	4	26	55.38	60.31	108.53	−2	3	30	66.77	77.89	141.91
2	4	26	104.34	111.84	199.55	0	3	30	14.37	12.43	129.27
−3	0	27	0.18	0.22	0.00	2	3	30	57.91	79.37	336.73
−1	0	27	132.85	137.53	180.00	−1	0	31	22.63	34.70	180.00
1	0	27	25.38	23.68	180.00	1	0	31	1.83	1.65	0.00
3	0	27	108.43	124.53	0.00	3	0	31	0.00	19.41	0.00
−3	1	27	55.39	74.06	139.96	−3	1	31	4.26	9.44	329.06
−1	1	27	55.52	51.65	48.22	−1	1	31	61.23	52.74	31.90
1	1	27	73.70	78.81	316.19	1	1	31	18.25	17.61	134.69
3	1	27	40.21	47.07	234.82	3	1	31	39.77	38.41	211.24
−3	2	27	7.76	17.05	10.54	−3	2	31	21.65	27.24	345.43
−1	2	27	51.92	58.57	281.14	−1	2	31	51.18	62.98	94.48
1	2	27	22.92	18.82	221.71	1	2	31	40.42	33.07	164.36
3	2	27	57.14	49.04	105.73	3	2	31	52.78	63.53	273.40
−3	3	27	36.16	46.67	230.94	0	0	32	206.61	186.05	0.00
−1	3	27	31.09	37.61	312.01	2	0	32	18.59	4.82	0.00
1	3	27	47.38	58.07	46.66	−2	1	32	144.70	166.10	322.02
−1	4	27	33.98	53.13	10.49	0	1	32	53.65	46.69	37.23
1	4	27	10.23	9.90	316.11	2	1	32	158.30	165.59	140.99
0	0	28	12.40	9.16	180.00	−2	2	32	10.35	10.63	223.35
2	0	28	20.27	14.94	0.00	0	2	32	79.81	87.53	105.18
4	0	28	0.00	2.56	0.00	2	2	32	24.94	16.15	354.81
−4	1	28	5.97	18.79	255.91	0	3	32	62.18	18.18	315.66
−2	1	28	80.62	83.59	142.35	−1	0	33	11.94	12.35	180.00
0	1	28	29.78	22.41	36.91	1	0	33	44.46	56.34	0.00
2	1	28	80.26	81.98	322.41	−1	1	33	36.96	38.23	329.92
4	1	28	52.88	25.92	184.15	1	1	33	80.91	77.85	227.06
−2	2	28	9.59	30.09	10.47	−1	2	33	25.48	30.56	193.56
0	2	28	116.93	131.12	270.63	1	2	33	29.89	27.22	79.52
2	2	28	34.06	33.19	169.38	−2	0	34	43.60	33.18	0.00
−2	3	28	66.34	74.82	238.39	0	0	34	12.51	29.56	0.00
0	3	28	59.46	69.40	164.82	−2	1	34	6.99	9.92	133.13
2	3	28	61.18	68.27	59.05	0	1	34	15.26	16.16	343.62
0	4	28	30.10	32.05	13.43	0	2	34	57.95	56.09	189.74
−1	0	29	19.55	21.83	0.00	−1	0	35	35.24	49.33	0.00
1	0	29	44.67	47.10	0.00	−1	1	35	37.49	39.05	201.71